

Effect of processing parameters on the electrochemical performance of graphene/ nickel ferrite (G-NF) nanocomposite

Elham Kamali Heidari^{1,2}, Abolghasem Ataie^{1*}, Mahmoud Heydarzadeh Sohi¹, Jang Kyo Kim²

1. School of Metallurgy and Materials Engineering, College of Engineering, University of Tehran, Iran

2. Department of Mechanical and Aerospace Engineering, Hong Kong University of Science and Technology, Hong Kong

Received: 7 March 2015 ; Accepted: 19 May 2015

*Corresponding Author Email: aataie@ut.ac.ir, Telephone: +98 21 82084084, Fax: +98 21 88006076

Abstract

Fuel cells, secondary batteries and capacitors are among many promising energy storage devices. In particular, supercapacitors have attracted much attention because of their long life cycle and high power density. Graphene/nickel ferrite(G-NF) based supercapacitors were successfully fabricated through a one-step facile solvothermal route. Effects of synthesis conditions i.e. solvothermal time and temperature, on the powder particle characteristics were evaluated using x-ray photoelectron spectroscopy (XPS), powder x-ray diffraction (XRD) and high-resolution transmission electron microscopy (HRTEM). Fast Fourier transformation (FFT) patterns were also recorded on the HRTEM microscope to determine the lattice and crystallinity of the nanocomposites. Structural and chemical studies proved that increasing the solvothermal duration and temperature leads to improved crystallinity of NiFe_2O_4 phase as well as higher degree of reduction of graphene oxide to graphene. The electrochemical measurements showed that solvothermal conditions of 180°C and 10h produces the highest specific capacity of 312 and 196 F g^{-1} at current densities of 1 and 5 A g^{-1} , respectively calculated from charge-discharge test. This G-NF electrode material, also showed a capacity of 105 F g^{-1} after 1500 cycles at current density of 10 A g^{-1} which makes it an outstanding supercapacitor material with promising long cycle electrochemical stability and performance.

Keywords: *graphene, nanocomposite, NiFe_2O_4 , solvothermal, supercapacitor.*

1. Introduction

Fuel cells, secondary batteries, and capacitors are among many promising energy storage devices. In particular, supercapacitors have attracted much attention because of their long life cycle and high power density. Electrochemical energy storage mechanism in

supercapacitors (SCs) may be of electrical double layer (EDLC) or pseudocapacitive behavior. Electrical double layer capacitors (EDLC) operate in a double layer formed on the electrode surface, which limits the specific capacitance and leads to lower energy density

relative to their theoretical value. In contrast, pseudocapacitors using the oxidation–reduction reaction provide 3–4 times higher capacitance as they not only react at the surface but also near the surface of the active electrode [1-4].

Designing and fabricating novel structured active materials with enhanced energy density, long cycling life and high power operation is one of the key factors that render SCs' wide application in portable appliances and electronic vehicles. Although conducting carbon polymer pseudocapacitors have an environmentally benign nature, low cost, a high voltage window and high storage capacity, their practical usage is limited due to swelling and shrinkage of the conducting polymer during charging/discharging cycles which causes degradation of the electrode and fade-out of electrochemical performance. Compared to carbon materials, metal oxides have higher energy density and better stability [5]. For example, hydrous RuO_2 supercapacitors show superior electrochemical properties such as high proton conductivity and a highly reversible redox process [4, 6], but they suffer from high material cost and often exhibit poor cycling stability (amorphous MnO_2 supercapacitors) [7-9]. Nickel oxide (NiO) or nickel hydroxide (Ni(OH)_2), cheap and environment-friendly alternatives have very high theoretical capacitances of 2584 and 2082 F g^{-1} respectively. However, according to literature, the typical specific capacitance based on nickel electrode ranges from 50 to 1634 F g^{-1} [10-11]. Ferrites, with chemical formula of MFe_2O_4 , where M is Fe, Mn, Ni, and Co are a new class of pseudocapacitive oxides. The capacitances are in the order of $\text{MnFe}_2\text{O}_4 > \text{CoFe}_2\text{O}_4 \gg \text{NiFe}_2\text{O}_4, \text{Fe}_3\text{O}_4$ [12].

Recently, a combination of carbon materials and metal oxides such as $\text{MnO}_2/\text{graphene}$ [13], $\text{NiO}/\text{graphene}$ [14], $\text{CO}_3\text{O}_4/\text{graphene}$ [15] amongst others have attracted attention because such composite active electrode materials benefit from the advantages of both components; superior conductivity and large surface area of carbon materials along with high specific capacitance of metal oxides [16].

Here in, a facile low temperature

solvothermal method for synthesizing G-NF nanocomposites as an active material electrode for supercapacitors is reported. The effect of process parameters such as solvothermal time and temperature on supercapacitor performance of the material are also investigated.

2. Materials and Methods

2.1. Synthesis of G-NF nanocomposites

Graphene oxide (GO) was prepared using a chemical method based on our previous work [17]. 0.5 g expanded graphite was mixed with 100ml H_2SO_4 stirred for half an hour and then 5g KMnO_4 was gradually added to the mixture and stirred at 60°C for 24 h. The solution was then transferred into an ice bath and deionised water (DI) and H_2O_2 were poured slowly into the mixture resulting in a color change of the suspension to light brown. After stirring for 30 min, GO was washed three times using HCl aqueous solution followed by washing with DI water until the pH of the solution became about 5–6. The GO obtained was re-dispersed in ethanol or water (as desired) at a concentration of 2 mg ml^{-1} .

Figure 1 shows a schematic of the synthesis of the G-NF composites. The stoichiometric ratio of the precursors to GO, in order to reach a nanocomposite with 60% GO, were determined according to our previous research [17]. To prepare G-NF nanocomposites containing 60 wt% of graphene, 0.141 g $\text{Fe(NO}_3)_3 \cdot 9\text{H}_2\text{O}$ (Sigma Aldrich) and 0.0511 g $\text{Ni(NO}_3)_2 \cdot 9\text{H}_2\text{O}$ (Sigma Aldrich) were initially mixed with 60 ml GO dispersion and the mixture was then vigorously stirred, followed by a drop-wise addition of NH_3 to adjust the pH of the mixture to about 10 and stirred for 1h. The resulting mixture was transferred into a Teflon-lined stainless steel autoclave and heated to 120 or 180°C at different time periods between 10 and 20h. After solvothermal treatment, the autoclave was allowed to cool down to ambient temperature and the product was washed with water and ethanol several times followed by drying at 60°C in a vacuum oven.

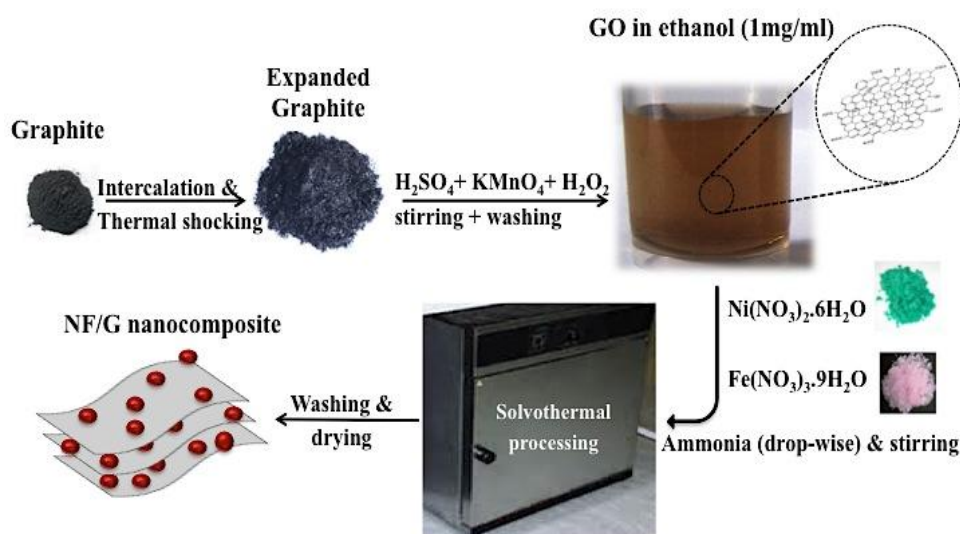


Fig. 1. Schematic drawing of the synthesis of the G-NF composites

2.2. Characterization

X-ray photoelectron spectroscopy (XPS, Surface analysis PHI5600, Physical Electronics) was employed to evaluate the chemical states of the nanocomposites using Al K α line as the excitation source. The phase structure of the nanocomposites was determined on a powder X-ray diffraction (XRD) system (PW1830, Philips) with Cu K α radiation from 10 to 90°. The morphology of the nanocomposite samples was examined using high-resolution transmission electron microscopy (HRTEM, JEOL 2010) at 200 kV. Fast Fourier transformation (FFT) patterns were also recorded on the HRTEM microscope to determine the lattice and crystallinity of the nanocomposites.

2.3. Electrochemical measurements

The working electrode was prepared by mixing the active material, carbon black and polyvinylidene fluoride (PVDF) in a weight ratio of 70: 10: 20. A few drops of N-methyl-2-pyrrolidone (NMP) as the solvent was added to form a proper slurry which was coated onto a nickel foam.

A beaker-type 3-electrode system with Na_2SO_4 1M aqueous electrolyte was used to measure electrochemical properties at room temperature. Ag/AgCl and Pt were used as reference and counter electrode, respectively. Cyclic voltammetry (CV) test was performed on an electrochemical workstation (CHI 660C)

within a potential range from -0.9 to +0.1 V versus Ag/AgCl electrode at different scan rates of 10, 20, 30, 40, 50 and 100 mV s^{-1} . Galvanostatic charge-discharge tests were carried out at different current densities of 1, 2, 3, 4 and 5 mA g^{-1} within a potential window of -0.9 to +0.1 V. Electrochemical impedance spectroscopy (EIS) was carried out in a frequency range of 100 kHz to 0.1 Hz at a fixed perturbation amplitude of 5 mV. The specific capacities were calculated based on the weights of the active material.

3. Results and Discussion

Figure 2 shows the XRD patterns of the G-NF nanocomposites synthesized using different solvothermal conditions. The diffraction peaks in all samples were identical and consistent with NiFe_2O_4 , indicating virtually no effect of graphene substrate on the crystalline structure of NF nanoparticles. The peak of 26.5° in samples prepared at 120°C for 10 and 16 h (Figs. 2a and b) is related to the graphitic structure, which disappeared after prolonged treatment at higher temperatures. During hydrothermal treatment, graphene oxide is reduced to graphene and graphene sheets are very likely to re-stack. Although this re-stacking is inhibited by nucleation and growth of NiFe_2O_4 nanoparticles in-between the sheets, at a low solvothermal temperature and time, particles are not well nucleated and grown in-between the sheets and so the graphitic peak is observed. The

disappearance of this peak at longer times and higher temperature arises from the disordered stacking of graphene sheets due to the growth of NF particles [18]. The generally broadened peaks for the nanocomposites are a reflection of the formation of very fine NiFe_2O_4 nanocrystals. The nanocomposites synthesized at 120°C show a more amorphous structure than those prepared at 180°C . Furthermore, increasing the solvothermal duration from 10 to 20 h at similar temperature resulted in sharper peaks as a consequence of the improvement in crystalline structure.

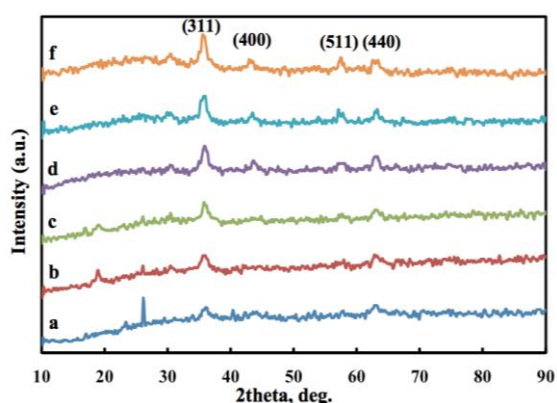


Fig. 2. XRD patterns of G-NF nanocomposites synthesized (a) at 120°C for 10 h; (b) at 120°C for 16 h; (c) at 120°C for 20 h; (d) at 180°C for 10 h; (e) at 180°C for 16 h; and (f) at 180°C for 20 h.

Figure 3 shows the XPS spectra of the nanocomposites synthesized under different conditions. The Ni 2p XPS spectra (Fig. 3a) exhibited two peaks at 852.5 and 870.2 eV which are assigned to Ni $2p_{3/2}$ and Ni $2p_{1/2}$, respectively [19]. Two peaks Fe $2p_{3/2}$ and Fe $2p_{1/2}$ were found to be 711.6 and 725.1 eV (Fig. 3b) representing the existence of Fe^{3+} and the formation of NiFe_2O_4 , respectively [19]. To determine the degree of reduction of GO under different processing conditions, the corresponding deconvoluted C1s spectra of GO-NF before and after selected solvothermal processes are shown in Figure 3c. The spectra obtained before the treatment exhibited four peaks at 284.6, 286.2, 288.0 and 289.5 eV, corresponding to carbon atoms with different oxygenated functional groups: namely, non-oxygenated C, C–O, C=O and O–C=O, respectively [20]. Regardless of processing conditions, the peak intensities of oxygenated functional groups in the samples after

treatment were much lower than those of the GO-NF obtained before treatment, confirming effective reduction of GO.

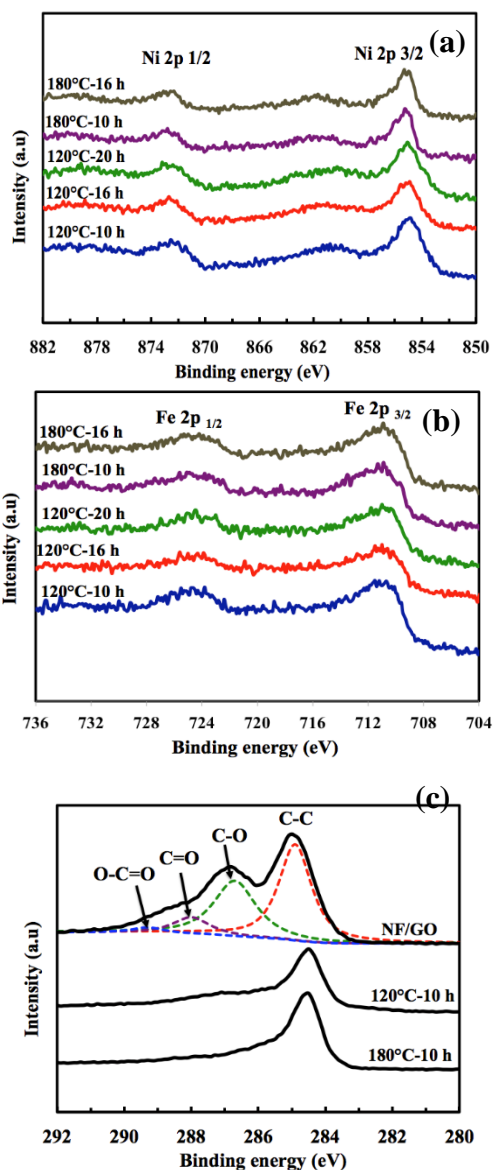


Fig. 3. (a) Ni 2p XPS spectra, (b) Fe 2p XPS spectra of nanocomposites at different synthesis conditions, and (c) deconvoluted C1s spectra of nanocomposites before solvothermal treatment and after solvothermal processes at 120°C and 180°C for 10 h.

Figure 4 shows a comparison between HRTEM images and the corresponding fast Fourier transformation (FFT) patterns of the G-NF nanocomposites with different solvothermal conditions. According to TEM images (Fig. 4 a, c and e), the particles are well dispersed on the surface of graphene sheets with an average size of 7 nm. In order

to clarify the lattice planes of NF, FFT patterns of related HRTEM images were studied as shown in Figure 4b, d and F. The reciprocal value of the distance between each bright dot and the centre of the FFT pattern is the d-spacing of a plane. These values were measured using GATAN digital micrograph demo software and then compared with spinel NiFe_2O_4 lattice d-spacings. The FFT pattern of G-NF synthesized at 120°C for 10h (Fig. 4b) showed amorphous structures. Increasing the time to 20 h led to emergence of lattice fringe spacing of 0.25 nm well matched with (311) planes of NiFe_2O_4 (Fig. 4d). More lattice fringes could be seen in FFT pattern related to

the sample synthesized at 180°C for 10h (Fig. 4f). The lattice fringe spacings of this sample measured from FFT pattern (Fig. 4f) were 0.25, 0.29, 0.24 and 0.21 nm which match with (311), (220), (222) and (400) planes respectively, of NiFe_2O_4 nanoparticles. Therefore, it could be concluded that increasing synthesis temperature from 120 to 180°C led to an obvious improvement in crystalline structure. This observation is valid even with a short solvothermal time of 10 h indicating the importance of synthesis temperature more than the process duration for the formation of NF nanocrystals, which also agrees with the XRD patterns.

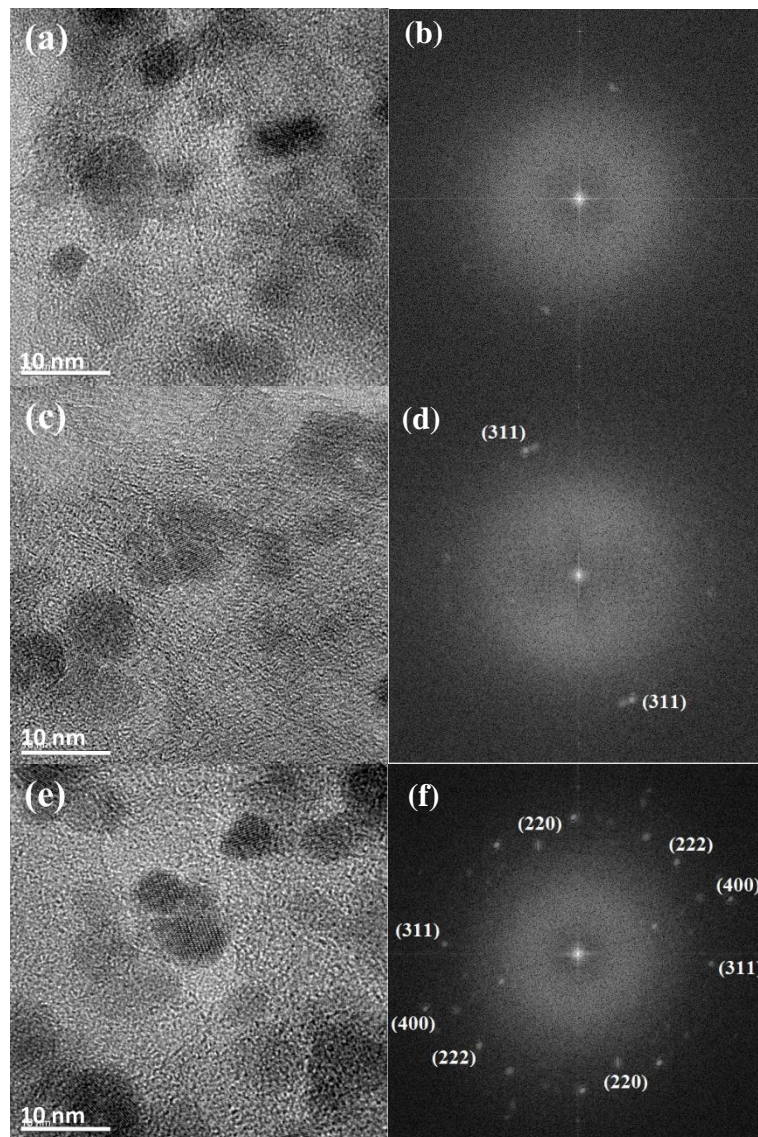


Fig. 4. (a) HRTEM images and the corresponding FFT patterns of G-NF nanocomposites synthesized at (a, b) 120°C for 10 h; (c, d) 120°C for 20 h; and (e, f) 180°C for 10 h.

Charge- discharge (CV) and EIS measurements have been carried out to investigate the electrochemical behaviors of the obtained G-NF nanocomposites. Figure 5 shows the galvanostatic charge-discharge curves of G-NF electrodes synthesized at different process parameters in a current density of 1 A g^{-1} . In nanocomposites prepared at 120°C , the highest capacity is obtained in the sample heated for 16h (Fig. 5 a). However, increasing the temperature to 180°C leads to a change in capacity as the highest values results from the sample prepared at the lowest solvothermal time of 10 h (Fig. 5 b).

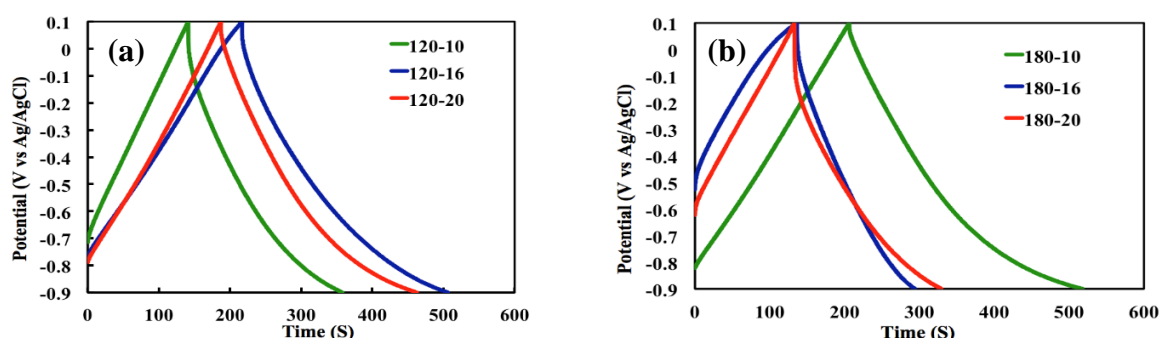


Fig. 5. Galvanostatic charge-discharge curves of G-NF composites synthesized at (a) 120°C and (b) 180°C for different time durations, at current density of 1 A g^{-1}

Table 1. Specific capacity calculated based on charge–discharge graphs of the electrode materials

G:NF	Solvothermal Temp ($^\circ\text{C}$), Time (h)	S-Capacity (F/g)				
		1A/g	2A/g	3A/g	4A/g	5A/g
60:40	120, 10	218	166	126	100	90
60:40	120, 16	290	237	182.4	159.2	143.5
60:40	120, 20	275	244	201	179	152
60:40	180, 10	312	262	233	222	196.2
60:40	180, 16	267	210.4	167.7	144.8	127
60:40	180, 20	196	140	96.9	73.6	55

The highest capacitance for G-NF nanocomposites synthesized at all current densities is at 180°C for 10 h. This electrode has a capacity of 312 and 195 F g^{-1} at current densities of 1 and 5 A g^{-1} , respectively. The good electrochemical performance of G-NF synthesized at 180°C for 10 h can be attributed to appropriate experimental conditions leading to less aggregation of graphene sheets and

The accurate specific capacitance (C_s) of all electrodes was calculated from the galvanostatic discharge curves based on Eq. 1 [21].

$$C_s = It / m. \Delta V \quad (1)$$

where m (g) is the mass of active material, I (A) is the current density, ΔV (V) is the potential window and t is the discharge time. Table 1 lists the charge–discharge data of the electrode materials calculated from the above equation at different current densities.

good dispersion of NiFe_2O_4 nanoparticles on the surface of graphene, thus leading to a higher active surface area for charge storage. Although 180°C is an appropriate temperature which results in crystalline nanoparticles, the lowest capacity is for the electrode synthesized at 180°C for 20h. It is assumed that increasing processing time leads to growth and agglomeration of nanoparticles

and a decrease in surface area and consequently results in worse electrochemical properties of this electrode.

Second high capacity electrodes are nanocomposites synthesized at 120°C for 20 and 16 h. According to TEM images, although NiFe₂O₄ nanoparticles are well dispersed on the surface of graphene sheets at 120 °C and 10h, the poor crystallinity or possible existence of some intermediate phases might be responsible for lower electrochemical performance. Increasing the time to 20h leads to structural improvement at this temperature.

Electrochemical capacities of the electrodes were also studied using cyclic voltametry. Figure 6 (a) shows CV curves of all nanocomposites at scan rate of 10 mV s⁻¹. The area in between each CV curve is directly related to the specific capacity. Thus according to the area between the CV curves, it can be seen that CV curve of G-NF nanocomposites obtained at 180°C for 10 h is wider than for all other samples implying that it has the highest specific capacity. A comparison between all curves in this figure shows that these results are in good agreement with the capacities calculated from charge-discharge curves meaning that

nanocomposites synthesized at 120 °C for 20 and 16 h are in the second place in terms of high specific capacity. The lowest capacities are for the nanocomposites synthesized at 180°C for 20 and 16 h, respectively.

The irregular-shaped rectangular CV curves in all electrodes indicate complex supercapacitance, namely pseudocapacitance and EDLC. Pseudocapacitance behavior is due to the existence of NiFe₂O₄ nanoparticles in the composites. However, regarding the fact that graphene is the dominant component of the composites (Wt.% G: NF = 60:40), the whole curves tend to have a rectangular shape which is a characteristic of EDLCs. CV curve of the nanocomposite synthesized at 120 °C for 10 h is an oxidative redox reaction. Such peak disappears with increasing solvothermal temperature or time. Therefore, it might be due to the oxidation of some functional groups on the surface of graphene or any probable interphases rather than NiFe₂O₄ which is removed after prolonged solvothermal time or higher temperature. The CV curves of G-NF synthesized at 180 °C for 10h at different scan rates of 10, 20, 30, 40, 50 and 100 mV s⁻¹ are shown in Figure 6 b.

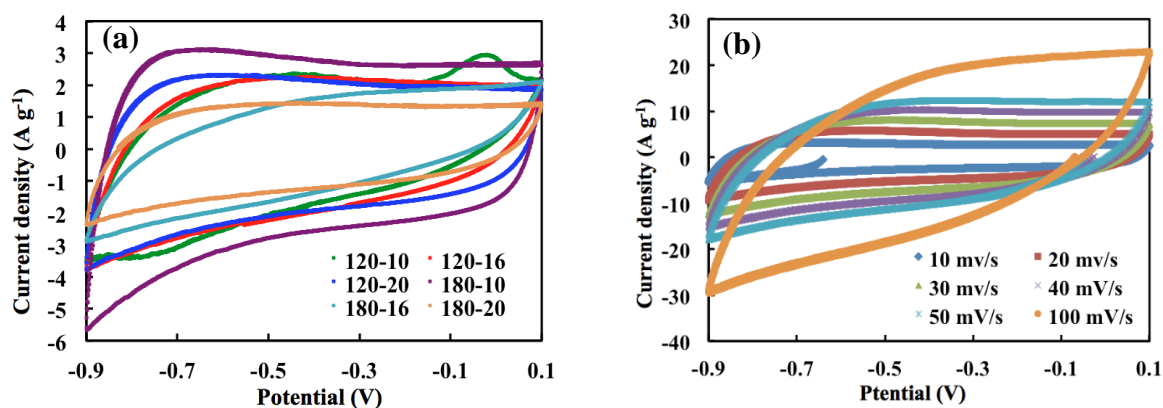


Fig. 6. (a) CV curves of G-NF electrodes synthesized at different process conditions, at scan rate of 10 mV s⁻¹, (b) CV curves of G-NF electrodes synthesized at 180 °C for 10h at different scan rates of 10, 20, 30, 40, 50 and 100 mV s⁻¹.

Figure 7 shows the EIS measurements of nanocomposites prepared at the aforementioned synthesis parameters. According to the semi-circles of Nyquist plots in Figure 7a, the lowest electron conductivity in nanocomposites prepared at 120°C is at the lowest solvothermal treatment time. EIS curves of nanocomposites treated at 180°C for

different durations show the same trend as well (Fig. 7b). The highest electron conductivity is obtained for nanocomposite prepared at 180°C for 20h. This might be due to the reduction degree of graphene oxide during the solvothermal process. Actually, one important phenomenon in the solvothermal process of graphene oxide is the removal of

oxygen containing functional groups from its surface there by rendering a more pure graphene which is the main responsible component of electron conductivity of nanocomposites. This fact is already well proved by XPS measurements in Figure 3, which shows increasing time and temperature leads to decrease or removal of oxygen containing functional group peak intensities. In contrast to graphene oxide, graphene has very high electron conductivity and so higher solvothermal temperature or time produces more graphene rather than graphene oxide and therefore higher electron conductivity.

To study the electrochemical stability of the supercapacitor material synthesized in this research, charge discharge test was carried out on the best electrode (G:NF, 180°C, 10h) at high current density of 10 mA g⁻¹ (potential range from -1 to 0 V) for 1500 cycles (Fig. 8). According to the results, the capacity becomes stable after the 100th cycle and the prepared electrode has a capacity of 105 F g⁻¹ after 1600 cycles which is a higher capacity reported by Wang *et al.* [18] on the same system. Such a stable capacity after long cycles proves the stability of the nanocomposite active material.

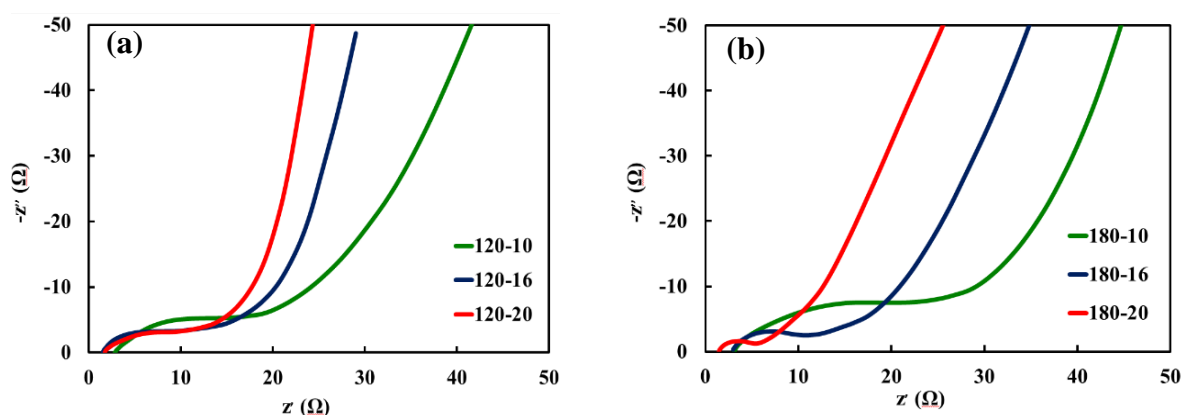


Fig. 7. The EIS Nyquist plot of nanocomposites prepared at (a) 120 °C and (b) 180 °C for different durations of 10, 16 and 20 h.

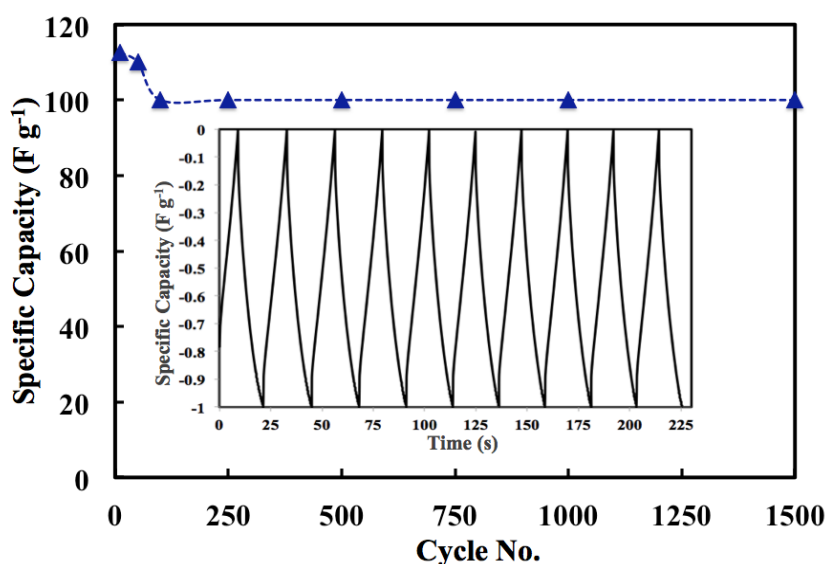


Fig. 8. Long cycle performance of G-NF (60:40) synthesized at 180 °C, 10h, at current density of 10 A g⁻¹ (charge-discharge curves for first 10 cycles inset)

4. Conclusions

G-NF based supercapacitors were fabricated through a one-step facile solvothermal route and the effect of process parameters was investigated on electrochemical capacitance of the electrodes. Electrochemical measurements showed that solvothermal conditions of 180 °C and 10h produced the highest specific capacity of 312 and 196 F g⁻¹ at current densities of 1 and 5 A g⁻¹, respectively calculated from charge-discharge test. Increasing solvothermal time at this temperature led to degradation of electrochemical performance which is due to particles agglomeration, and therefore reduction of the surface area. The second high capacity electrodes were those prepared at 120°C for 16 and 20h, meaning that 10h is not enough for crystallization of the NiFe₂O₄ nanoparticles at 120°C. G-NF electrode materials, synthesized at 180°C, 10h showed a capacity of 105 F g⁻¹ after 1500 cycles at current density of 10 A g⁻¹ which makes it an outstanding supercapacitor material with promising long cycle electrochemical stability.

References

- [1]. Jagadale, A.D., Kumbhar, V.S., Dhawale, D.S., Lokhande, C.D., *Electrochimica Acta* vol. 98, 2013. pp. 32-38.
- [2]. Lee, J.S., Lee, C., Jun, J., Shin, D.H., Jang, J., *J. Mater. Chem. A*, vol. 2, 2014. pp. 11922-11932.
- [3]. Wang, W., Guo, S., Lee, I., Ahmed, K., Zhong, J., Favours, Z., Zaera, F., Ozkan, M., Ozkan, S., *Sci. reports*, vol. 4, 2014. pp.4452.
- [4]. Li L., Loveday, D.C., Mudigonda, D.S.K., Ferraris, J.P.J., *Electrochem. Soc. Vol.* 149, 2002. pp. 1201-1207.
- [5]. Xie, X., Zhang, C., Wu, M.B., Tao, Y., Lvac, W., Yang, Q.H., *Chem. Commun. Vol.* 49, 2013. pp. 11092-11094.
- [6]. Wang, W., Guo, S., Lee, I., Ahmed, K., Zhong, J., Favours, Z., Zaera, F., Ozkan, M., Ozkan, C. S., *Scientific Reports*. vol. 4, 2014. pp. 24452, 1-9.
- [7]. Liang, K., Tang, X., Hu, W., *J. Mater. Chem.* vol.22, 2012. pp. 11062-11066.
- [8]. Kim, H., Popov, B. N., *J. Electrochem. Soc.* vol.150, 2003. pp. 56-62.
- [9]. Chen, S., Zhu, J., Wu, X., Han, Q., X. Wang, *ASC Nano*.vol.4, 2010. pp. 2822-2830.
- [10]. Yan, X., Tong, X., Wang, J., Gong, C., Zhang, M., Liang, L., *J. Alloy. Compd. Vol.* 593, 2014. pp. 184-189.
- [11]. Li, M., Xu, W., Wang, W., Liu, Y., Cui, B., Guo, X., *J. Power Sources*. vol. 248, 2014. pp. 465-473.
- [12]. Zhang, L. L., Zhao, X. S., *Chem. Soc. Rev.* vol. 38, 2009. pp. 2520-2531.
- [13]. Bello, A., Fashedemi, O. O., Lekitima J. N., Fabiane M., Arhin D. D., Ozoemena K.I., Gogotsi Y., Johnson A. T. C., Manyala N., *AIP Advances*. vol.3, 2013. pp.0821181-0821189.
- [14]. Zhao, B., Song, J., Liu, P., Xu, W., Fang, T., Jiao, Z., Zhang, H., Jiang, Y., *J. Mater. Chem.* vol. 21, 2011. pp. 18792-18798.
- [15]. Lee, J.S., Lee, C., Jun, J., Shin, D. H., Jang J., *J. Mater. Chem. A*. vol. 2, 2014. pp.11922-11929.
- [16]. Kassaei, M.Z., Motamedi, E., M. Majidi, *Chem. Eng. J.* vol. 172, 2011. pp. 540-549.
- [17]. Kamali Heidari, E., Zhang, B., Heydarzadeh Sohi, M., Ataie, A., Kim, J.K., *J. Mater. Chem A*. vol.2, 2014. pp. 8314-8322.
- [18]. Wang, Z., Zhang, X., Li, Y., Liu, Z., Hao, Z., *J. Mater. Chem. A*. vol.1, 2013. pp. 6393-6399.
- [19]. Fu, M., Jiao, Q., Zhao, Y., *J. Mater. Chem. A* vol. 1, 2013. pp. 5577-5586.
- [20]. Moulder, J. F., Stickle, W. F., Sobol, P. E. Bomben, K.D. (Inc., Eden Prairie, MN, USA, *Handbook of X-ray Photoelectron Spectroscopy*, Physical Electronics 1995.
- [21]. Xiang, C., Li, M., Zhi, M., Manivannan, A., Wu, N., *J. Power Sources*. Vol. 226, 2013. pp. 65-70.